Open access • Journal Article • DOI:10.1260/136943307780150850

Layered Finite Element Analysis of One-Way and Two-Way Concrete Walls With Openings — Source link

Philip Hallinan, Hong Guan

Institutions: KBR, Griffith University

Published on: 01 Feb 2007 - Advances in Structural Engineering (SAGE Publications)

Topics: Ultimate load

Manuscript submitted to

Advances in Structural Engineering – An International Journal

LAYERED FINITE ELEMENT ANALYSIS OF ONE-WAY AND TWO-WAY CONCRETE WALLS WITH OPENINGS

by

Philip Hallinan, **Hong Guan**

September 2006

Layered Finite Element Analysis of One-Way and Two-Way Concrete Walls With Openings

Philip Hallinan[a], H. Guan[b,*]

[a]*Kellogg Brown & Root Pty Ltd, 555 Coronation Drive, Toowong, Queensland, Australia*

[b]*Griffith School of Engineering, Griffith University Gold Coast Campus, PMB50 Gold Coast Mail Centre, Queensland, Australia*

Abstract

Empirical wall design equations provided in major codes of practice are conservative because they do not cover walls that are supported on all four sides or walls with slenderness ratios greater than 30. They do not cover walls that require openings for doors, windows and services. The recognition of such factors in design codes would result in savings in construction costs. This study investigates the effect of side restraints and the presence of openings for reinforced concrete wall panels where axial load eccentricity induces secondary bending. A numerical analysis of such walls is undertaken using the non-linear Layered Finite Element Method (LFEM), and results are compared with eight one-third to one-half scale wall panels tested previously at Griffith University. The LFEM predicts the failure loads, the load-deflection responses, the deformed shapes and the crack patterns of the tested wall panels. Subsequent parametric studies on the ultimate load carrying capacity of 54 one-

* Corresponding author. Tel.: +61 7 5552 8708; fax: +61 7 5552 8065.
E-mail address: h.guan@griffith.edu.au

way and two-way reinforced concrete walls with openings established relationships of failure load with slenderness ratio and eccentricity.

Keywords: finite element analysis, concrete walls, openings, restraint conditions, slenderness ratio, eccentric load, code methods

1. Introduction

Reinforced concrete wall panels are becoming more popular as load bearing structural members rather than simply being used as a defence against environmental elements. Recent research on tilt-up precast panels and the increased use of reinforced concrete core walls in high-rise construction has increased the popularity of load bearing reinforced concrete wall construction worldwide. More often than not concrete walls require openings for doors and windows in tilt-up construction and for services and safety reasons in core walls used for high-rise construction. The presence of these openings cause large tensile stresses, particularly around opening corners which affect the structural behaviour of the wall inducing premature cracking and limiting its load carrying capacity.

Currently the design of reinforced concrete wall panels under eccentric axial loading is carried out using empirical or semi-empirical methods. Although concrete codes devote separate chapters to the design of walls, the limited research on this type of structural member means that code provisions such as the Australian Concrete Standard AS3600 (2001) and the American Concrete Institute code ACI-318 (2005) are often conservative. In addition these codes are limited to one-way action (walls supported at the top and bottom only), slenderness ratios less than 30 (in AS3600) and 25 (in ACI-318), are only for normal strength concrete (20-65 MPa), and do not allow for openings. Two-way walls (walls supported on all four sides by adjoining walls or columns) are commonly found in practice as core walls or shear walls and have the effect of substantially increasing the load capacity of a wall panel. Furthermore current design codes allow only minimal strength for slender wall panels (where the height over thickness ratio $H/t_w > 30$), although experimental work has proven this not to be the case, particularly if the slender panel is supported in two-way action. Substantial

reductions in construction costs could be realised if design codes allowed practicing engineers to design structural members that take advantage of the strength gains of two-way wall supports.

Many researchers such as Saheb and Desayi (1989, 1990a), and Doh and Fragomeni (2004), have over the past one to two decades investigated the behaviour of solid concrete wall panels in either one-way or two-way action. Much of this research has focussed on wall panels that are under eccentric axial loading and are supported top and bottom only (one-way action). These walls behave as a column in compression where the deformation is characterised by uniaxial curvature in the direction of loading. A lesser amount of research has been conducted on walls supported on all four sides (two-way action), which behave as a transversely loaded slab where biaxial curvatures occur in the directions parallel and perpendicular to that of loading (Doh and Fragomeni 2004). Although research has given insight into many different types of walls, two areas are identified as having limited information and are the focus of this study. The first area is concrete walls with openings as required for doors and windows in tilt-up construction, and for services and safety reasons in core walls. An accurate design of concrete walls with openings is particularly difficult due to the non-uniform loading which is induced surrounding the openings. The second area is walls with high slenderness ratios. The increased popularity of high strength concrete and advances in concrete technology have resulted in thinner walls being employed in high-rise and tilt-up construction and hence there is a need to investigate the behaviour of load bearing slender wall panels.

For concrete walls with openings under axial eccentric loading, much of the research conducted to date has been based on experimental work (Zielinski et al. 1982; Saheb and

Desayi 1990b; Doh and Fragomeni 2006), the outcomes of which are a series of empirical formulas. Over the past ten years numerical simulation and computer analysis of concrete wall behaviour has become more popular, however many numerical studies utilising commercial finite element packages have had mixed results (Al-Mahaidi and Nicholson 1997; Raviskanthan et al. 1997; Fragomeni 1998). Recently efforts in using the specialised nonlinear Layered Finite Element Method (Loo and Guan 1997; Guan and Loo 1997) for the analysis of one-way and two-way concrete walls without an opening have produced promising results (Doh et al. 2001; Guan and Loo 2002).

In this study the LFEM is applied for the first time to one-way and two-way walls with openings. In a comparative study the LFEM predicts the failure load, the load-deflection response, the deformed shape and the crack patterns for eight one-third to one-half scale wall panels with openings which were previously tested at Griffith University by Doh and Fragomeni (2004). The establishment of a benchmark model enabled further parametric studies on a total of 24 wall panels investigating slenderness ratio, and 30 wall panels investigating the effects of eccentricity on the ultimate load capacity of one-way and two-way concrete walls with openings. Relationships of failure load with slenderness ratio and eccentricity are subsequently established.

2. Methodology - nonlinear Layered Finite Element Method (LFEM)

The nonlinear Layered Finite Element Method (LFEM) is identified as a suitable means of analysis that is expected to yield satisfactory results and take into consideration openings, one- and two-way action, high slenderness ratios and a range of eccentricities in concrete walls. The LFEM was originally developed for the punching shear failure analysis of horizontal structural members such as flat plates and slabs (Loo and Guan 1997; Guan and

Loo 1997). It simplifies the three-dimensional elasticity to a shell situation (Polak 1998) by using degenerate shell elements each consisting of multiple fully bonded layers. Each layer contains gauss points at its mid-surface where the stresses which are assumed to be uniform over the layer thickness are computed. This creates a stepwise approximation of the stress distribution over the thickness of the element (the wall thickness t_w) which is illustrated in Fig. 1.

The LFEM encompasses three-dimensional (in-plane and out-of-plane) stress components in its finite element formulation and is thereby capable of analysing both flexural and shear cracking up to failure. It considers both geometric and material non-linearities. The aim of the layered model is to simulate plasticity over the cross section of an element. The non-linear analysis implies that the material state at any Gauss point can be elastic, plastic or fractured depending on the loading history. The LFEM assumes that when the stress at the mid point of an outer layer reaches the specified yield stress, this outer layer becomes plastic while the remaining layers remain elastic. This process continues until all layers become plastic and the whole cross section yields.

In the LFEM, concrete failure is identified as a result of either tension cracking or plastic yielding (crushing). An elastic brittle fracture behaviour is assumed for concrete in tension. Cracks are assumed to form as soon as the principal tensile stress reaches the specified concrete tensile strength f_t. Crack direction is in the plane perpendicular to the tensile force. Cracked concrete is treated as an orthotropic material using a smeared crack approach and the tension cut-off representation is utilized. Due to the aggregate interlock and bond effects, both the shear stiffness deterioration (in terms of reduced shear moduli) and the

tension stiffening effect (due to bond effects between concrete and steel) are taken into consideration after the concrete is cracked.

The compressive behaviour of concrete is modelled using the strain-hardening plasticity approach which determines the boundaries of elastic and plastic regions (when the initial yield surface is attained) and the progress of damage in the plastic zone. When the compression type of failure transpires in concrete (when the ultimate strain ε_u is reached), some but not all strength and rigidity of the material is lost. This is represented by the effect of bulk modulus in the concrete material. Numerical modelling of either cracking or crushing of concrete involves the modification of material stiffness and partial or full release of the appropriate stresses in the fractured elements.

The reinforcing steel is assumed to be uniaxial elastic-plastic material. The reinforcing bars at a given level in an element are modelled as a smeared steel layer of equivalent thickness.

The total material matrix containing the contributions of concrete and steel can be determined for each element and the stiffness matrix for the corresponding element can be evaluated using the Gaussian integration technique where the selective integration rule is adopted. The global stiffness matrix is then assembled using the standard procedure. The Newton-Raphson method, an incremental and iterative procedure, is used to obtain the nonlinear solution due to both material and geometric non-linearities. The LFEM is capable of determining not only the load-deflection response and the ultimate load carrying capacity, but also the crack patterns and the deflected shape at any stage up to the failure load.

Fig. 2 illustrates a single layered finite element. The LFEM uses eight-node degenerate shell elements with five degrees of freedom specified at each nodal point. These are the in plane displacements (u and v respectively in the x and y directions), transverse displacement (w in the z direction), and two independent rotations about the x and y axes (θy and θx respectively).

The element is subdivided across its depth into eight concrete layers of varying thickness, with thinner layers towards the outer faces and thicker layers towards the centre of the wall. The primary objective of this is to improve the accuracy of the crack patterns on the outer faces. Steel reinforcement in the wall panel is placed centrally in the panel cross-section, and consists of a single layer of F41 mesh (4mm diameter steel bars at 100mm centres in both the x and y directions) (Doh and Fragomeni 2004). The steel mesh is modelled by smearing the total volume of steel in each direction across two perpendicular layers with equivalent thicknesses. This results in a total of 10 layers for each element. The concrete and smeared steel layers in a typical element are illustrated in Fig. 3.

3. Verification of finite element model with test results

3.1. The wall models

A total of eight wall panels tested previously by Doh and Fragomeni (2004) are used in the comparative study, four one-way and four two-way. The aspect ratio is equal to one for all panels. Amongst the eight panels, four distinct geometric wall configurations are used. These include two one-way wall panels, with one and two openings respectively, and two two-way wall panels with one and two openings also. These are illustrated in Fig. 4. The size

of each opening is equal to a quarter of the height (H) or the width (L) for all wall panels. Openings are placed centrally for walls with one opening and symmetrically for walls with two openings. The wall thickness (t_w) for all wall panels regardless of their size is equal to 40 mm, and the load eccentricity (e) is $t_w/6$ (where the axial distributed load is offset from the centreline of the wall). The value of H and L varies giving different slenderness ratios as summarised in Table 1. Also shown in Table 1 are the opening size and the concrete compressive strength for each panel. The yielding strength of steel is 450 MPa for all the panels. Note that the minimum reinforcement, in accordance with the Australian Standard and the ACI code, is provided for all the panels to prevent shrinkage cracking during the curing period. Due to the small thickness of the wall panels, the steel mesh is placed centrally in the cross-section and is not considered as a structural component that can contribute to the out-of-plane behaviour of the wall panels. This is similar to practical situations where slender walls less than 100 mm thick are generally provided with minimum reinforcement placed centrally.

Due to symmetry only a quarter of each wall panel is modelled. A convergence study is conducted to determine the most appropriate mesh size for each model. The total number of nodes and elements determined from the convergence study is also given in Table 1. With mesh sizes as shown the solution accuracy is high and little improvement can be made by introducing additional nodes and elements. A typical finite element mesh for panel TW12 is presented in Fig. 5 showing the refined mesh in the region around the opening. Also shown in the figure is a set of equivalent nodal loads (concentrated forces and moments) applied along the top edge to reflect the eccentric axial load applied in the experimental work. For both one-way and two-way walls the test rig, along the top loaded edge, provides restraint against displacement in the z-direction and against rotation about the y-axis (see Fig. 2).

These degrees of freedom are restrained accordingly in the finite element model. For one-way wall panels the side edge is left unrestrained while for the two-way panels this edge is restrained against z-displacement and rotation about the x-axis (see Fig. 2). For the nodes on the right and bottom edges of the quarter model, the corresponding symmetrical restraint conditions apply.

3.2. One-way wall panels

In general the LFEM overestimated the ultimate load carrying capacity of one-way walls with a mean LFEM/Experimental failure load of 1.11 and a standard deviation of 0.17. A comparison of the failure loads, N_{uo}, is presented in Table 2. The deformation and cracking behaviour for all walls is relatively consistent and agreed with experimental observation.

The mean LFEM/Experimental failure load of 1.11 is expected as the LFEM is an idealistic model in which there is no variation in material and section properties. Such ideal conditions are rarely found in practice or even in the more controlled experimental work. The LFEM model idealises possible dimensional variations, material irregularities, concrete voids, changes in reinforcement location, and the variations in restraint or loading conditions that may exist in experimental work and are even more likely to occur in normal construction conditions. These all have the effect in most cases of reducing the failure load of the wall panels in the experimental tests.

The load-deflection responses for the four panels are presented in Fig. 6. Some errors in the experimental setup can be clearly identified especially in the elastic zone. Figs. 7 and 8 show respectively the deformed shapes and a comparison of crack patterns (on the tensile

face) of two typical wall panels, OW11 and OW21. Note that the LFEM prediction of the crack pattern is for a quarter of each wall panel.

In Fig. 7 wall panels OW11 and OW21 clearly show one-way behaviour with maximum deflection occurring near the mid-height of the walls. In the beam section above the single opening of the one-way walls there appears to be a small amount of bending about the y-axis in addition to the major bending about the x-axis. This is due to the reduced stiffness above the opening caused by the void in the panel. For the one-way walls with two openings, forces from above the two openings are transferred to the central column section causing it to deform the most.

The crack patterns predicted by the LFEM for the one-way walls with one opening are well predicted showing the dominant horizontal crack direction as illustrated in Fig. 8. Note that the solid lines in the figure indicate only the crack direction at specific Gauss points and they do not offer information on crack length and width. The crack patterns for walls with two openings are also well predicted by the LFEM. There is a concentration of horizontal cracks near the mid-height of the wall similar to the experimental work and a number of vertical cracks are observed above the openings. Cracks appear to be initiated from the corners of openings where stress concentrations exist. A larger number of cracks spread over a greater area are displayed in the LFEM results compared with experimental observations. This is because in the LFEM a crack is displayed at any Gauss point at which the tensile strength of concrete (f_t) is exceeded regardless of the length or width of the crack. In the experimental work however, many of the smaller cracks are either not visible to the human eye or merge together forming a larger and more localised crack. Nevertheless together with

the deformed shape and load-deflection response, the ultimate strength and failure behaviour of the wall panels can be simulated satisfactorily by the LFEM.

3.3. Two-way wall panels

The LFEM predictions of failure load for two-way walls are different to those of the one-way walls. The failure load, N_{uo}, is underestimated for all the wall panels with a mean LFEM/Experimental failure load of 0.86 and a standard deviation of 0.11. This is shown in Table 3. For two-way walls the most significant explanation for the conservative nature of the LFEM predictions are the boundary conditions. The LFEM idealises the complex partial restraint conditions in the experimental work which contribute significantly to the strength of the walls. The results do show a high level of consistency however which enables a benchmark to be established. In the analysis, most panels demonstrated a load-deflection response similar to that of the experimental work, and in most cases results showed a more sudden failure than what is observed for the one-way panels.

The load-deflection responses for the four panels are presented in Fig. 9. Note that for panel TW21 an extra set of data is recorded at the mid point of the central column section of the wall. Figs. 10 and 11 show respectively the deformed shape and a comparison of crack patterns (on the tensile face) of two typical wall panels, TW11 and TW21.

The deformed shapes for panels TW11 and TW21 clearly display biaxial curvature which is typical for two-way action and similar to the shape observed in the experimental work. In two-way action the restrained edges obviously have no out-of-plane displacement, and maximum displacement occurs near the centre of the panel resulting in curvature in both

directions. For the walls with two openings the out-of-plane displacement of the central column region between the openings is considerably larger than other areas of the panel. This is because forces from above the openings are transferred to this central region which has no side restraint and subsequently behaves like a one-way wall.

In Fig. 11 crack patterns for two-way walls are much more widespread than their one-way equivalents in both the LFEM predictions and the experimental observations. For walls with one opening the main crack direction is from the corner of the opening to the nearest outer corner of the panel itself, consistent with the two-way curvature. The LFEM accurately predicts this crack behaviour. The LFEM also predicts extensive vertical cracking in the column section between the opening and edges of the panel. Both these cracking behaviour can be clearly observed in experimental work. For the two-way wall panels with two openings the crack patterns become more complex. The LFEM predicts cracks that propagate from the top edge and all corners of the openings. The crack direction is mainly towards the upper corners of the wall panel with many cracks also heading towards the upper loaded edge. There is no cracking to the left of the opening. These observations are similar to those made in the experimental work. One difference is that there is little cracking predicted by the LFEM in the central column region between the two openings. This is because in the experimental work the cracks in the central column appear suddenly just before the wall is collapsed. At this point in the numerical analysis the solution no longer converges meaning the wall is deemed to have failed just prior to the cracks being displayed by the LFEM.

In summary the LFEM has proved to be an effective modelling tool for simulating the behaviour of one- and two-way reinforced concrete walls with openings. Fig. 12 summarises the comparison of experimental results and LFEM predictions. The majority of data points lie

close to the line showing a strong correlation between the experimental and predicted failure loads. The exception is the wall panel TW12 whose data point has the only significant deviation from the 45 degree line. An examination of the experimental results reveals that the experimental failure load is about 300 kN greater than what would have been expected when comparing to other data. The discrepancy is attributed to experimental error such as an inadequate eccentricity being set, or reinforcement being placed off the centre. Furthermore during other analysis of the experimental data (Doh and Fragomeni 2004), this data point was consistently an outlier, even when plotted in other relationships. There is strong evidence to support disregarding this data point in the establishment of a benchmark. Hence the modelling techniques adopted in this comparative study are used for further investigation of slenderness ratio and eccentricity of loading.

4. Parametric study on slenderness ratio of wall panels

4.1. Ultimate load carrying capacity

The effect of the slenderness ratio on the ultimate load carrying capacity of reinforced concrete walls with openings is investigated herein. Four panel types (one-way, two-way, one opening, two openings) are studied in which the overall dimensions (H and L) are varied to achieve slenderness ratios (H/t_w) of 10, 15, 25, 30, 40 and 50. In total, 24 models are included in this parametric study. Amongst the 24 models, eight are equivalent to the panels examined in the comparative study. The geometric details are presented in Tables 4 and 5 respectively for one-way and two-way wall panels. The concrete strength is assumed to be the same as that for the two-way walls in the comparative study. The wall thickness, the reinforcement

configuration and its respective material properties remain the same as they are for the comparative study.

The failure loads N_{uo} are predicted by the LFEM for walls with slenderness ratios ranging from 10 to 50 and are presented in Tables 4 and 5 for one and two-way walls respectively. It is evident in Table 4 that for one-way walls with both one and two openings the failure load increases with slenderness ratio up to a point between the slenderness ratios of 25 and 30, after which it begins to decline. This behaviour is attributed to the change in failure mechanism from predominantly bending for stubby wall panels to buckling for more slender wall panels. The initial increased capacity of the wall panels is not due to the larger slenderness ratio itself, but rather the increased gross cross sectional area of the larger panels. Results illustrate that the gross cross sectional area has a large impact on the capacity of the wall when bending failure is dominant, however as the failure mechanism moves towards buckling its significance becomes smaller. For panels with slenderness ratios greater than 25, the increased strength obtained from the greater cross sectional area is more than offset by the increased instability of the more slender panels. It is important to note that the ACI-318 code limits the slenderness ratio to 25 for one-way walls, and the AS3600 code limits slenderness ratio to 30. The results presented herein reflect this limitation.

For two-way wall panels with both one and two openings, Table 5 indicates that failure loads do not cease to increase until slenderness ratios of approximately 40 to 50 are reached. This phenomenon is similar to one-way wall panels. The distinctive feature for two-way wall panels is that there exists additional stability provided by the side restraints and buckling behaviour does not become dominant until higher slenderness ratios are reached. This

appears to occur at a slenderness ratio of over 40 compared with 25 for the one-way wall panels.

Also included in Tables 4 and 5 are the normalised data, viz the axial strength ratio $N_{uo}/f_c^{'}Lt_w$, where N_{uo} is the predicted failure load for wall panels with openings; $f_c^{'}$ is the concrete compressive strength; L and t_w are respectively the width and thickness of the panel. The axial strength ratio eliminates the effects of changing panel size and concrete strength on the failure load of the panel. This dimensionless quantity is useful for comparing the behaviour of different wall panels. The axial strength ratio versus the slenderness ratio for the four wall types is plotted together in Fig. 13. From this plot the effect of slenderness ratio on the strength of each wall panel can be investigated. The overall trend for these wall panels is that as the panels become more slender the axial strength ratio is decreased; however the extent of this decreased strength varies between the four wall types. The two-way wall panels with both one and two openings clearly show a greater strength than their one-way equivalents. Furthermore, the panels with one opening clearly show a higher strength than those with two openings. At a slenderness ratio of 50 there is little difference between the axial strength ratio of the walls with one and two openings, however at low slenderness ratios this difference is significant. The gross cross sectional area which is directly influenced by the number of openings has a significant effect on the capacity of a wall failing in bending, and at low slenderness ratios bending failure is dominant. The number of openings and therefore the gross cross sectional area has a lesser effect on the buckling type failure of the more slender panels.

The results demonstrate that walls with slenderness ratios greater than the limits imposed by the design codes still have significant strength, particularly for walls supported on

all four sides. However the study has not considered the increased sensitivity of slender wall panels to lateral loads such as wind and earthquake, or loads during construction and should therefore be interpreted with caution.

A cubic relationship is identified in Fig. 14 between the slenderness ratio and the additional strength gained from the two-way restraints (in the form of the failure load ratio between two-way and one-way walls $N_{uo,TW}/N_{uo,OW}$). It is predicted however that a relatively accurate and simplified linear relationship can be established between these variables. A linear regression line is therefore fitted to the data as presented in Fig. 14. The R^2 value of 0.97 indicates a high correlation between the proposed linear relationship and the numerical results. This relationship can be utilised to great advantage in the development of a new design formula.

4.2. The proposed formula

The LFEM predictions of this parametric study are compared in Fig. 15 with available test data (Doh and Fragomeni 2004) and other predictions by empirical formulas (AS3600 2001; ACI-318 2005; Doh and Fragomeni 2006). Note that both the AS3600 and ACI-318 formulas are for walls without openings and the slenderness ratios H/t_w are limited to 30. In addition the experimental data of Doh and Fragomeni covers H/t_w of 30 and 40 only. Note also that the effective width of the panel, L_o (= L - opening width), is used in Fig. 15 to enable a comparison with AS3600 and ACI-318 which do not consider openings. The inadequacy of the national codes of practice is clearly identified in this figure.

The test data and the LFEM predictions both have an axial strength ratio significantly larger than that predicted by the national codes of practice. Furthermore these predictions are for walls with openings, and if a comparison was made for solid walls the conservative nature of the codes of practice would be even greater. The experimental work is well predicted by both the LFEM and the empirical formula of Doh and Fragomeni (2006). This is particularly true for the one-way walls where a strong correlation is demonstrated. For the two-way walls however this is only the case for H/t_w between 30 and 40. The Doh and Fragomeni's predictions become increasingly smaller than those of the LFEM for $H/t_w \leq 30$, but greater for $H/t_w \geq 40$. There have been numerous tests on one-way wall panels with H/t_w up to 30 which led to the development of the empirical methods adopted by AS3600 and ACI-318. However test data covering the full range of slenderness ratios for two-way wall panels is relatively limited. This may help to explain the discrepancies between the empirical and numerical methods in predicting the axial strength ratios outside the range of the test data. While more experimental testing is needed for two-way walls with openings, particularly those with H/t_w greater than 40 and less than 30, an attempt is made in this study to derive an empirical formula based on the numerical predictions.

Using the linear relationship between one-way and two-way walls as presented in Fig. 14, a modified empirical formula is proposed which predicts the failure load of two-way wall panels with openings. The new formula utilises the equation of Doh and Fragomeni (2006) who modified the AS3600 formula to predict the failure load of solid walls in one-way and two-way actions, and that of Saheb and Desayi (1990b) who considered the size and location of openings. The prediction of one-way wall panels will be considered in the same manner as proposed by Doh and Fragomeni (2006) which has already proven to give accurate results. To predict the failure load of a wall with two-way supports a restraint factor, λ, is introduced

into the equation. This factor multiplies the prediction made for a one-way wall panel to estimate the failure load of an equivalent two-way wall panel. From Fig. 14 and the equation of the regression line ($y = 0.038x + 1.04$) the λ factor is derived.

The proposed design formula for wall panels with openings is set out below:

$$N_{uo} = \lambda\ (k_1 - k_2\ \alpha)\ N_u \tag{1}$$

and from Doh and Fragomeni (2006),

$$N_u = 2.0 f'_c{}^{0.7}\ (t_w - 1.2e - 2e_a) \tag{2}$$

In Eqs. (1) and (2), N_{uo} and N_u are respectively the ultimate load of two identical wall panels with and without openings; λ is the restraint factor (λ = 1 and $\lambda = 0.038(H/t_w)+1.04$ for one- and for two-way wall panels, respectively); α is the reduction parameter which considers the size, number and location of openings (Saheb and Desayi 1990b), where in this study α = 0.25 and 0.5 for the walls with one and two openings respectively; k_1, k_2 are the constants derived from a calibration process where in this study k_1 = 1.188 and k_2 = 1.175 (Saheb and Desayi 1990b; Doh and Fragomeni 2006); e is the eccentricity of load; e_a is the additional eccentricity due to the out-of-plane deflection of the wall during loading (the P-delta effect), and $e_a = (H_{we})^2/(2500t_w)$ in which $H_{we} = \beta H$ and the effective height factor β = 1 for $H/t_w < 27$ and $\beta = \dfrac{18}{(H/t_w)^{0.88}}$ for $H/t_w \geq 27$.

By combining the restraint factor λ as determined in this study, with the published formulas by Saheb and Desayi (1990b), and Doh and Fragomeni (2006), a more accurate estimate of the failure load for two-way walls is achieved. The proposed formula is also simpler in its application. Only two k factors are required which are the same for both one and two-way walls, in comparison to the four factors required in the more complex method by Doh and Fragomeni (2006). Furthermore the tedious process of determining the effective height factor, β, for two-way walls has been eliminated and replaced by the factor λ which considers the effect of the two-way restraints.

4.3. Performance and limitations of the proposed formula

Table 6 compares the failure load predicted by the proposed formula $N_{uo,Proposed}$ using Eq. (1) with the LFEM predictions $N_{uo,LFEM}$ and the experimental results $N_{uo,Exp}$, for the 24 walls with openings in both one-way and two-way actions (as listed in Tables 4 and 5). The mean and standard deviations show that the proposed method gives satisfactory predictions.

Only limited data forms the basis of this comparison and more extensive test data is required to fully verify and validate the proposed formula. The major limitation of this method is that it has only been verified for walls with geometric properties similar to those in this study. Furthermore a major assumption is that the relationship between λ and H/t_w remains constant for all values of α (a factor dependant on the size and location of openings). This however has only been tested in this study for α of 0.25 and 0.5 for wall panels with one and two openings respectively. Moreover the effect of aspect ratio on the failure load of two-way walls with openings needs to be investigated before the formula can be applied to walls with an H/L value other than 1. Finally the LFEM that is used to derive the above formula

has been verified for only slenderness ratios of 30 and 40. Further verification of the LFEM is necessary for a wider range of slenderness ratios and wall types before a new formula such as that proposed is used with confidence.

5. Parametric study on load eccentricity of wall panels

5.1. Rationale

The parametric study of slenderness ratios has revealed a number of relationships, however these relationships are only observed for axial loading with an eccentricity of $t_w/6$ or 6.67 mm. The effect of load eccentricity e on slender concrete wall panels with openings is therefore investigated. Eccentricity is already included in many empirical design formulas, however in most cases these are only valid for slenderness ratios less than 30. This parametric study investigates the effect of eccentricity on wall panels with slenderness ratios H/t_w of 30, 40 and 50. The findings of this study combined with those of the parametric study on slenderness ratio can be used to produce design charts that consider a range of eccentricities for slender wall panels with openings. For each of the wall panels, eccentricities e of 0.05, 0.167, 0.3, 0.4 and 0.5 times t_w (=40 mm) are investigated. A total of 24 new models concentrating entirely on the two openings case and behaving in both one and two-way actions are analysed. Also included are the analysis results obtained in Section 4 of six one-way and two-way wall panels having H/t_w of 30, 40 and 50 and an eccentricity of 6.67 mm.

5.2. One-way wall panels

The failure loads as predicted by the LFEM are presented in Table 7. Results for one-way wall panels all follow a similar trend. For each different sized wall a steady decrease in failure load is evident as the eccentricity is increased. Additionally the maximum deflection decreases as the eccentricity of the load increases. The results also illustrate how the failure load of a panel with a large eccentric loading is a small fraction of the equivalent panel with a small load eccentricity.

Fig. 16(a) illustrates the relationship between the eccentricity and the failure load for panels in one-way action with slenderness ratios of 30, 40 and 50. The losses in strength with initial increases in eccentricity appear to be greater than subsequent losses as illustrated by the concave nature of the curves. Moreover the slenderness ratio appears to have a significant effect on the failure load when eccentricity is small, however only a minimal effect at higher eccentricities.

The fact that the lines on Fig. 16(a) are not smooth, and in one case cross over shows that numerical errors have occurred while reaching a solution. The most likely cause is due to the solution diverging just prior to failure for some wall panels. Although these errors exist they are relatively small and the results still give a good indication of wall behaviour under eccentric axial loading.

5.3. Two-way wall panels

The eccentricity has a significant effect on the failure load for the two-way wall panels also, as presented in Table 8. Similar to the one-way walls, significant decreases in failure load are observed as the eccentricity is increased.

Fig. 16(b) illustrates the effect of eccentricity on the failure load of two-way wall panels with slenderness ratios of 30, 40 and 50. The trend shown in this illustration is slightly different to that observed for the one-way walls. The relationship between the failure load and the eccentricity appears to be close to linear, however failure load still clearly decreases with increasing eccentricity.

5.4. Comparison

From the comparison of results it can be concluded that eccentricity has a greater effect on one-way walls than it does for two-way walls. Eccentricity induces out-of-plane bending making eccentric loading more significant for one-way wall panels where there is little resistance to these deflections. For the two-way walls side restraints provide support against out-of-plane bending helping to reduce the effects of eccentricity.

The parametric study illustrates the significant effect that load eccentricity has on the failure load of a wall panel. For one-way walls the strength of a panel with an eccentricity of $t_w/2$ is about 15% of that of the equivalent panel loaded with an eccentricity of $t_w/20$. For two-way walls this value is 22%, which although a slightly larger fraction is still an extremely significant design consideration.

6. Conclusions

To date there are only limited studies available for reinforced concrete walls with openings, walls supported on all four sides, and walls with high slenderness ratios. This paper focussed on the numerical analysis of axially loaded reinforced concrete walls with openings and slenderness ratios between 10 and 50 in which load eccentricity induces out-of-plane bending.

The non-linear Layered Finite Element Method (LFEM) has been used successfully in this study to give reliable predictions of overall load-deflection behaviour, crack patterns and deformed shapes for both one- and two-way concrete walls with openings. Satisfactory results are achieved in a comparative study between LFEM predictions and experimental test results. On average the LFEM overestimated the failure load of one-way wall panels and underestimated the failure load of two-way wall panels.

The parametric study on slenderness ratio revealed that as a wall panel becomes more slender its axial strength ratio decreases. It is also found that openings have a greater effect on the axial strength ratio at low rather than high slenderness ratios. A linear relationship is identified between the strength gains of having two-way restraints and the slenderness ratio. This relationship is used to derive a new parameter, λ, which considers the additional strength provided by the side restraints. This factor which demonstrates the benefits of two-way action is a useful outcome of this study, however before it can be put to any practical use the effect of different opening configurations will need further investigation. The formula by Doh and Fragomeni (2006) for one-way walls is modified to include the restraint factor λ, and

a simplified formula is produced that could be readily accepted in engineering design offices. The proposed design equation, although simpler to use than the two-way wall equation proposed by Doh and Fragomeni (2006), may neglect the effects of aspect ratio and the size and location of openings on the strength gains of using two-way wall panels. It is also important to note that the formula does not consider out-of-plane loading such as earthquake and wind which would need to be considered separately if designing slender wall panels using the proposed formula. A comparison of the formula with available test data and LFEM predictions, show that it satisfactorily predicts the failure load of reinforced concrete walls with openings.

A second parametric study showed that load eccentricity has a significant effect on the failure load of reinforced concrete walls with openings. In general greater eccentricities reduce the load capacity of a wall. Results also showed that eccentricity has a greater effect on one-way walls than it does for two-way walls.

Although a number of conclusions have been reached, much of the work is based on, and compared with a limited amount of experimental test data. There is scope for future research to fully verify the methods used and conclusions drawn from this study. More experimental test data for walls with slenderness ratios of 30 to 50, and walls with different opening configurations and aspect ratios should be collected to further verify the LFEM. The LFEM could then be used to investigate a wide range of wall properties and develop detailed design charts that consider factors such as those covered in this paper. It is anticipated that further research in this area will help eliminate the restrictions of current design codes and refine alternative empirical and analytical analysis techniques.

References

Al-Mahaidi, R. and Nicholson, K. (1997). "Nonlinear FE analysis of RC wall panels with openings", *Proceedings of the Fifteenth Australasian Conference on the Mechanics of Structures and Materials*, R.H. Grzebieta, et al. eds., Melbourne, Australia, December, pp. 449-454.

American Concrete Institute (ACI) (2005). *Building code requirements for reinforced concrete (ACI 318-05) and commentary - ACI318R-05*, Detroit, Michigan.

Doh, J.H. and Fragomeni, S. (2004). "Evaluation and experimental work for concrete walls with openings in one and two-way action", *Proceedings of the Third Civil Engineering Conference in the Asian Region*, S.W. Hong and H. Woo, eds., Seoul, Korea, August, pp. 307-310.

Doh, J.H. and Fragomeni, S. (2006). "Ultimate load formula for reinforced concrete wall panels with openings", *Advances in Structural Engineering*, Vol. 9, No. 1, 2006, pp. 103-115.

Doh, J.H., Fragomeni, S. and Loo, Y.C. (2001). "Investigation into the behaviour of reinforced concrete wall panels by finite element method", *Proceedings of the ICCMC/IBST 2001 Advanced Technologies in Design, Construction and Maintenance of Concrete Structures*, U. Taketo and T.D. Nguyen, eds., Hanoi, Vietnam, March, pp. 99-105.

Fragomeni, S. (1998). "Finite element analysis of reinforced concrete walls", *Proceedings of the Sixth East Asia-Pacific Conference on Structural Engineering and Construction*, Y.B. Yang and L.J. Leu, eds., Taipei, Taiwan, January, pp. 259-264.

Guan, H. and Loo, Y.C. (1997). "Flexural and shear failure analysis of reinforced concrete slabs and flat plates", *Advances in Structural Engineering*, Vol. 1, No. 1, pp. 71-85.

Guan, H. and Loo, Y.C. (2002). "Deflection, cracking and failure analysis of planar continuum reinforced concrete structures", *CD-ROM Proceedings of the Second International Conference on Advances in Structural Engineering Mechanics*, C.K. Choi and W.C. Schnobrich, eds., Pusan, Korea, August, pp. 1-8.

Loo, Y.C., and Guan, H. (1997). "Cracking and punching shear failure analysis of RC flat plates", *Journal of Structural Engineering*, ASCE, Vol. 123, No. 10, pp. 1321-1330.

Polak, M.A. (1998). "Shear analysis of reinforced concrete shells using degenerate elements", *Computers & Structures*, Vol. 68, No. 1-3, pp. 17-29.

Raviskanthan, A., Al-Mahaidi, R. and Sanjayan, J.G. (1997). "Nonlinear finite element analysis of slender HSC walls", *Proceedings of the Fifteenth Australasian Conference on the Mechanics of Structures and Materials,* Grzebieta, et al. eds., Melbourne, Australia, December, pp. 455-460.

Saheb, S.M. and Desayi, P. (1989). "Ultimate strength of RC wall panels in one-way in-plane action", *Journal of Structural Engineering, ASCE*, Vol. 115, No. 10, pp. 2617-2630.

Saheb, S.M. and Desayi, P. (1990a). "Ultimate strength of R.C. wall panels in two-way in-plane action", *Journal of Structural Engineering, ASCE*, Vol. 116, No. 5, pp. 1384-1402.

Saheb, S.M. and Desayi, P. (1990b). "Ultimate strength of RC wall panels with openings", *Journal of Structural Engineering, ASCE*, Vol. 116, No. 6, pp. 1565-1578.

Standards Association of Australia (SAA) (2001). *AS3600-2001: Concrete structures*, Sydney, Australia.

Zielinski, Z.A., Troitsky, M.S. and Christodoulou, H. (1982). "Full-scale bearing strength investigation of thin wall-ribbed reinforced concrete panels", *ACI Structural Journal*, Vol. 79, No. 32, pp. 313-331.

Table Legends

Table 1. Details of wall panels and convergence study results

Table 2. Comparison of experimental and LFEM failure loads for one-way walls

Table 3. Comparison of experimental and LFEM failure loads for two-way walls

Table 4. Summary of failure load N_{uo} for one-way wall panels

Table 5. Summary of failure load N_{uo} for two-way wall panels

Table 6. Comparison of failure load N_{uo}

Table 7. Summary of eccentricity and failure load for one-way walls

Table 8. Summary of eccentricity and failure load for two-way walls

Figure Captions

Fig. 1. Stress distribution of the layered model

Fig. 2. A single 8-node degenerate layered shell element

Fig. 3. Concrete and smeared steel layers in a typical element

Fig. 4. Four different configurations for wall panels

Fig. 5. Finite element mesh for quarter of wall panel TW12

Fig. 6. Load-deflection response for one-way wall panels

Fig. 7. Deformed shapes of OW11 and OW21

Fig. 8. Comparisons of tensile face crack patterns in OW11 and OW21

Fig. 9. Load-deflection response for two-way wall panels

Fig. 10. Deformed shapes of TW11 and TW21

Fig. 11. Comparison of tensile face crack patterns in TW11 and TW21

Fig. 12. Comparison of experimental and LFEM failure loads

Fig. 13. The effect of slenderness ratio on the axial strength ratio

Fig. 14. Relationship between H/t_w and additional strength gained from two-way restraints

Fig. 15. Comparison of LFEM results with other available data

Fig. 16. Effect of eccentricity on failure load of wall panels

Notation

e	=	Eccentricity of axial load
e_a	=	Additional eccentricity due to out-of-plane deflection
f'_c	=	Concrete compressive strength
f_t	=	Concrete tensile strength
H	=	Height of wall panel
k_1, k_2	=	Constants
L, L_o	=	Total and effective widths of wall panel
N_{uo}, N_u	=	Failure load of wall panels with and without openings
t_w	=	Thickness of wall panel
u, v, w	=	Displacements in the x, y and z directions
α	=	Reduction parameter for opening
ε_u	=	Concrete ultimate strain
θx, θy	=	Rotations about the x and y directions
β	=	Effective height factor
λ	=	Restraint factor

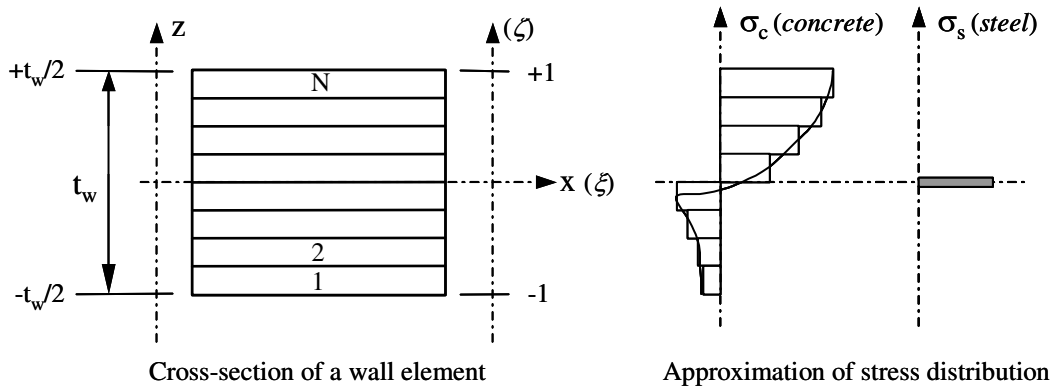

Figure 1. Stress distribution of the layered model

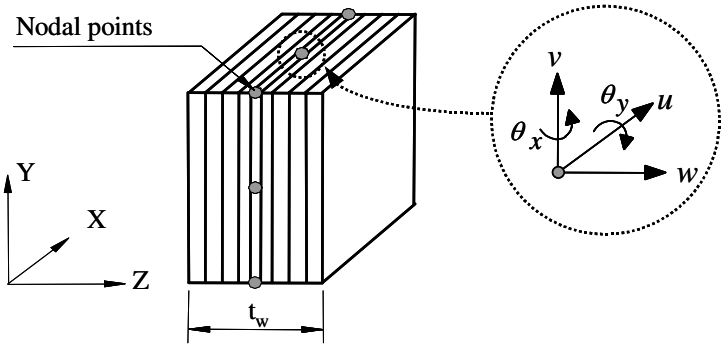

Figure 2. A single 8-node degenerate layered shell element

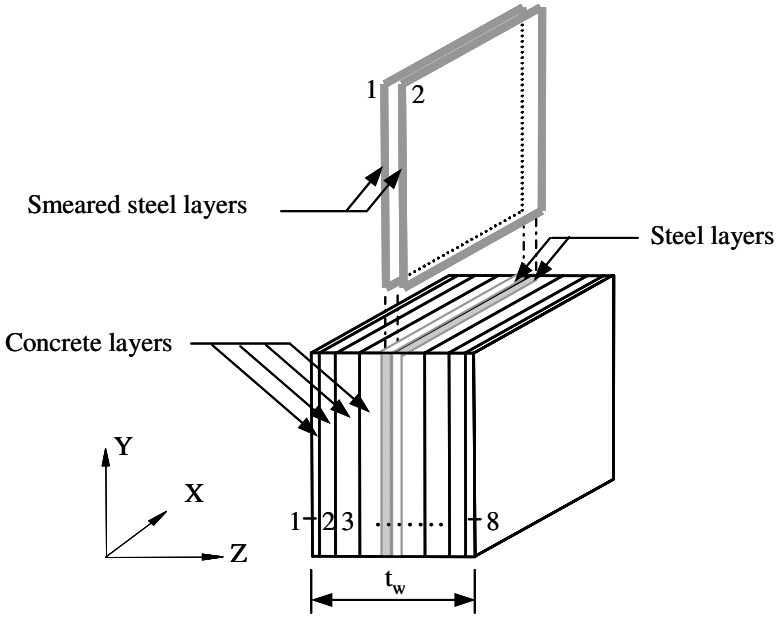

Figure 3. Concrete and smeared steel layers in a typical element

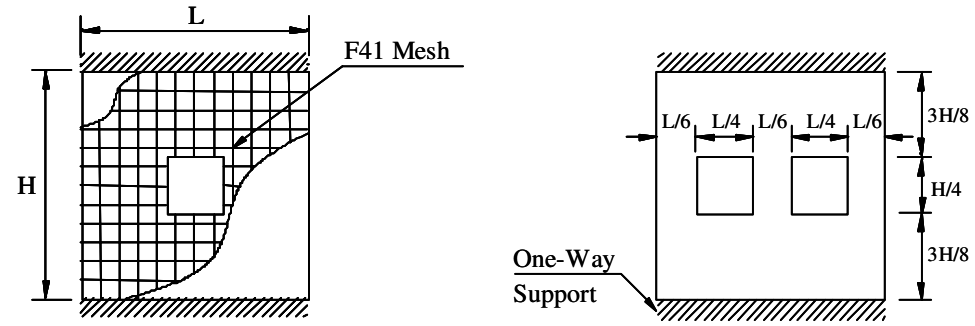

(a) One-way wall panels with one and two openings

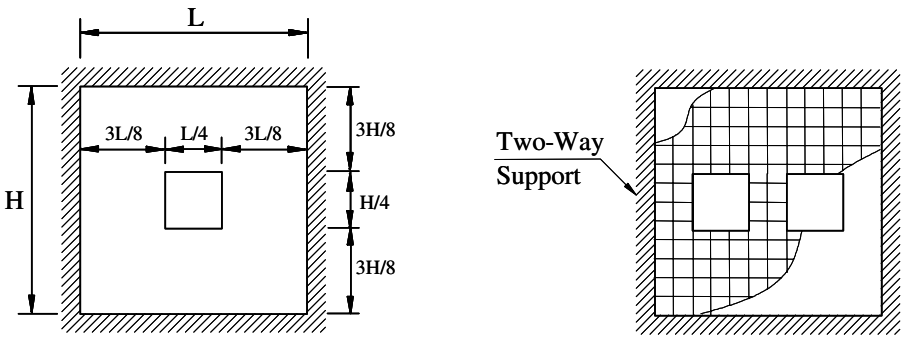

(b) Two-way wall panels with one and two openings

Figure 4. Four different configurations for wall panels

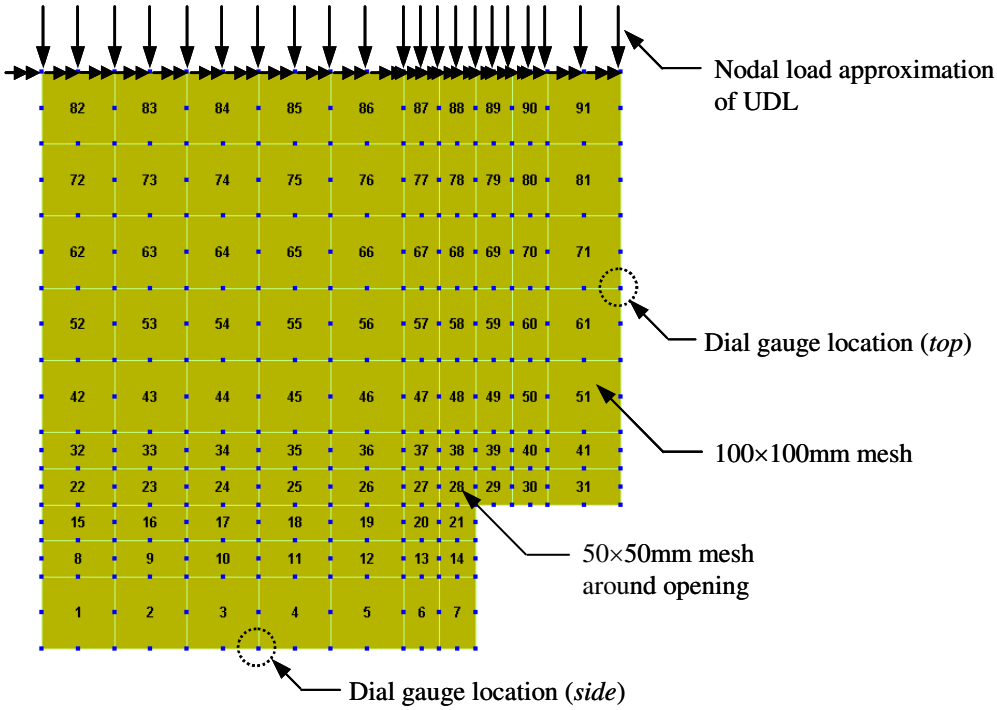

Figure 5. Finite element mesh for quarter of wall panel TW12

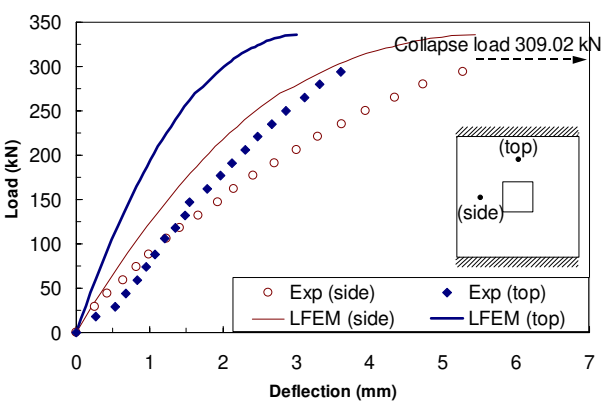

(a) OW11

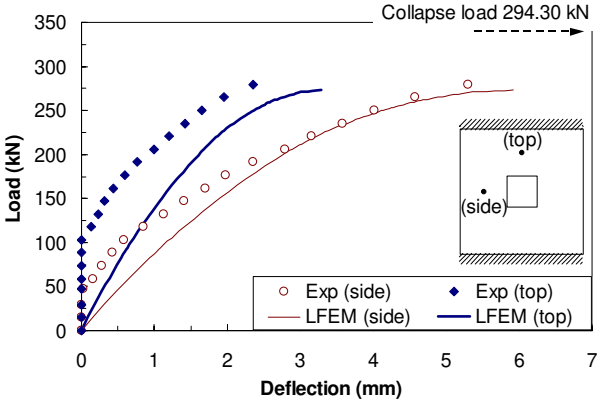

(b) OW12

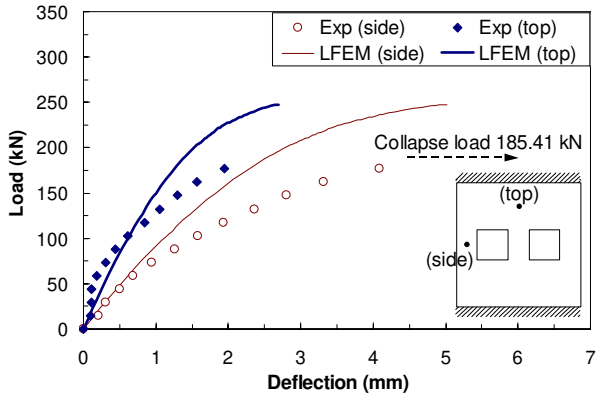

(c) OW21

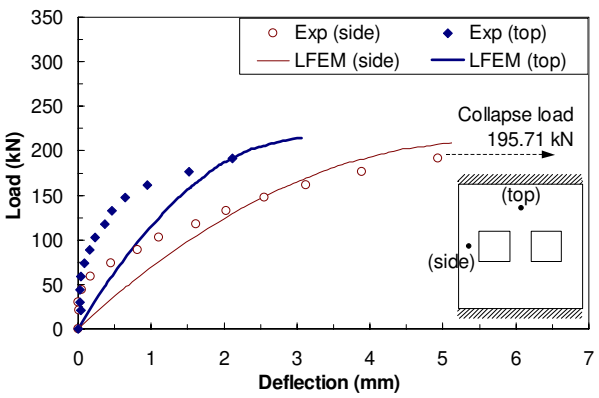

(d) OW22

Figure 6. Load-deflection response for one-way wall panels

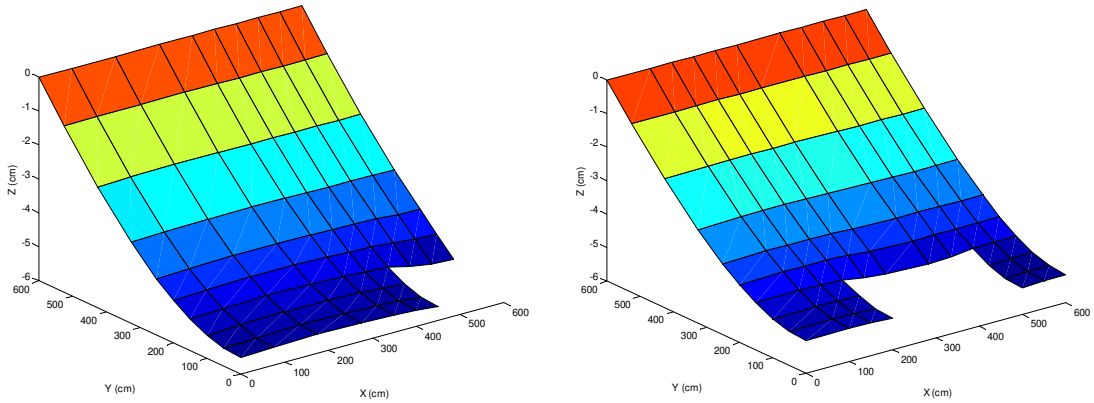

(a) OW11 (b) OW21

Figure 7. Deformed shapes of OW11 and OW21

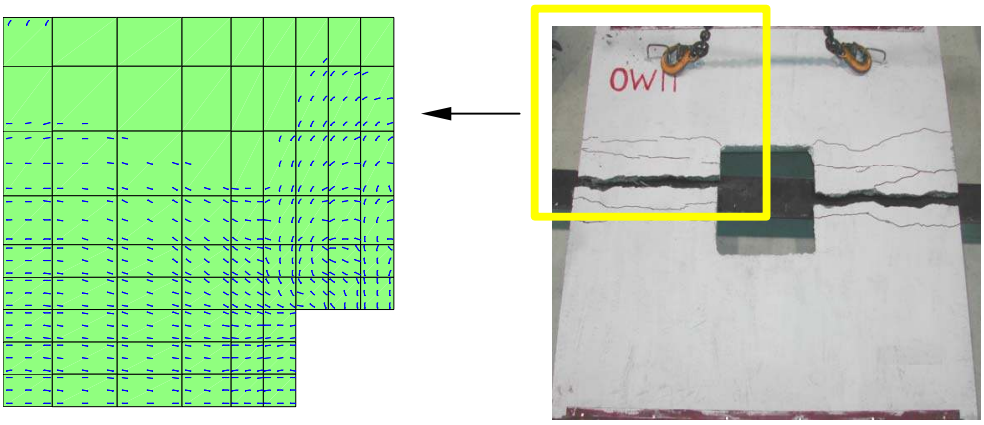

LFEM Experiment

(a) OW11

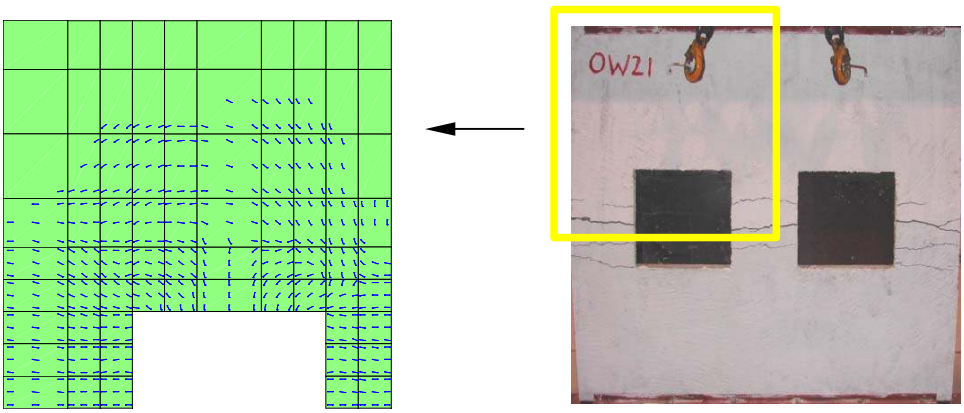

LFEM Experiment

(b) OW21

Figure 8. Comparisons of tensile face crack patterns in OW11 and OW21

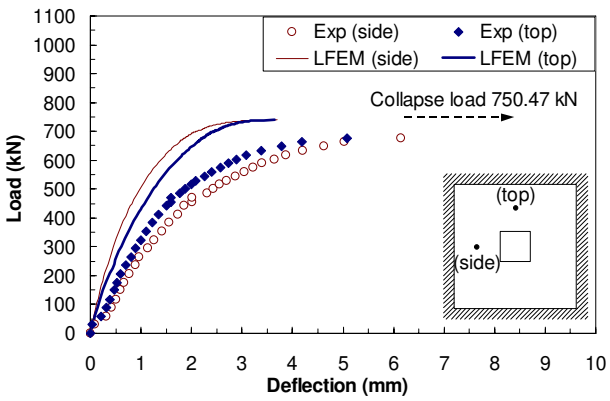

(a) TW11

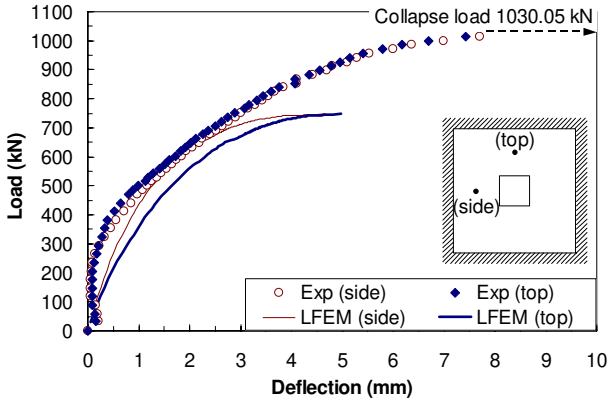

(b) TW12

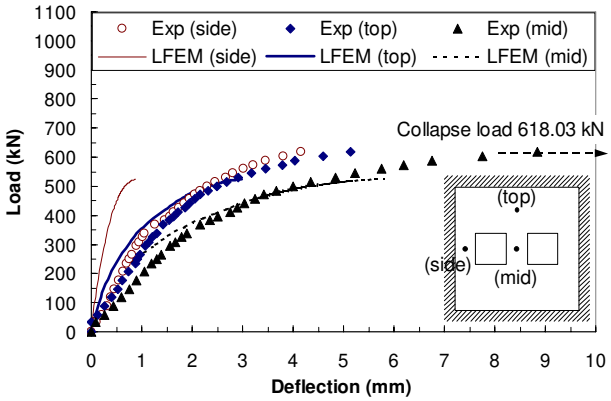

(c) TW21

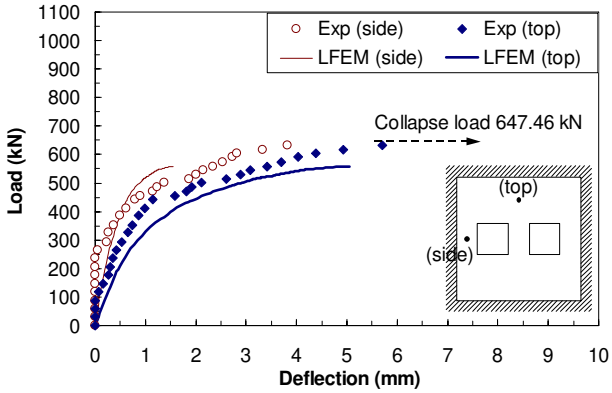

(d) TW22

Figure 9. Load-deflection response for two-way wall panels

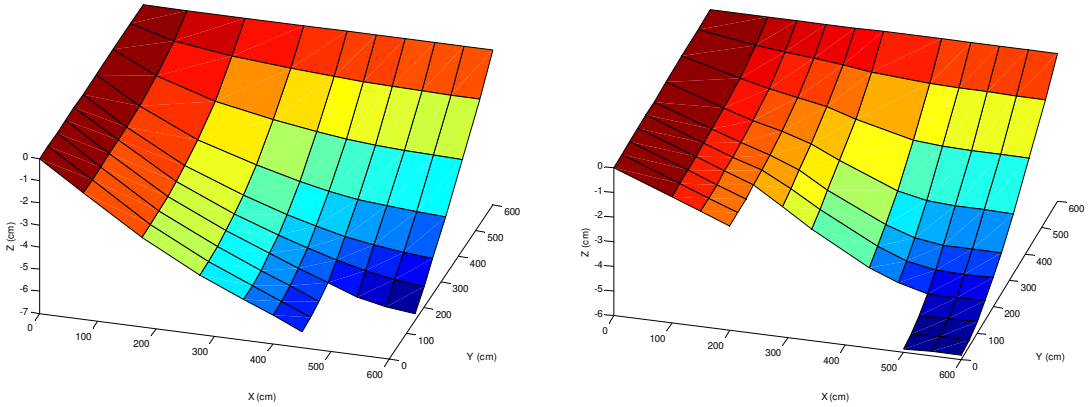

(a) TW11 (b) TW21

Figure 10. Deformed shapes of TW11 and TW21

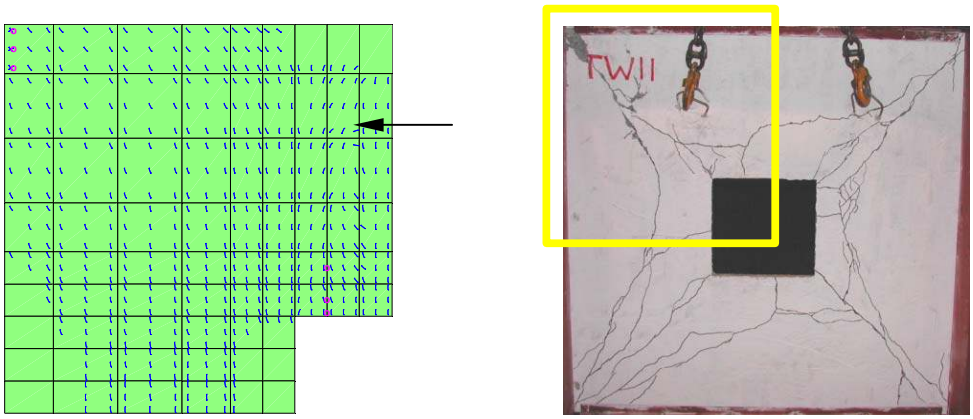

LFEM Experiment

(a) TW11

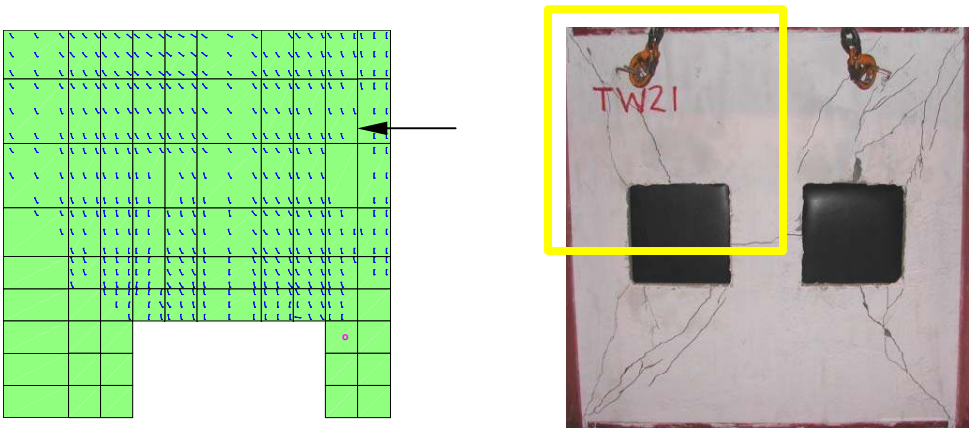

LFEM Experiment

(b) TW21

Figure 11. Comparison of tensile face crack patterns in TW11 and TW21

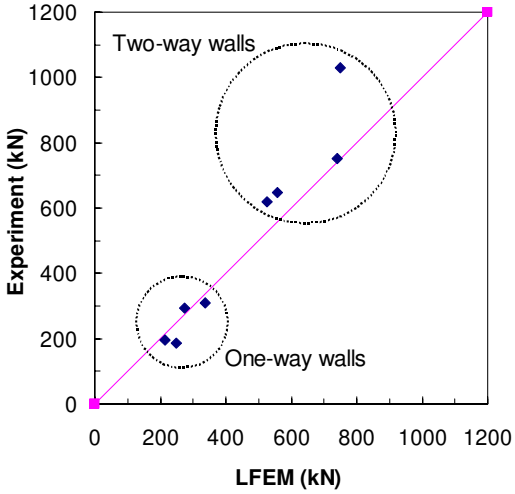

Figure 12. Comparison of experimental and LFEM failure loads

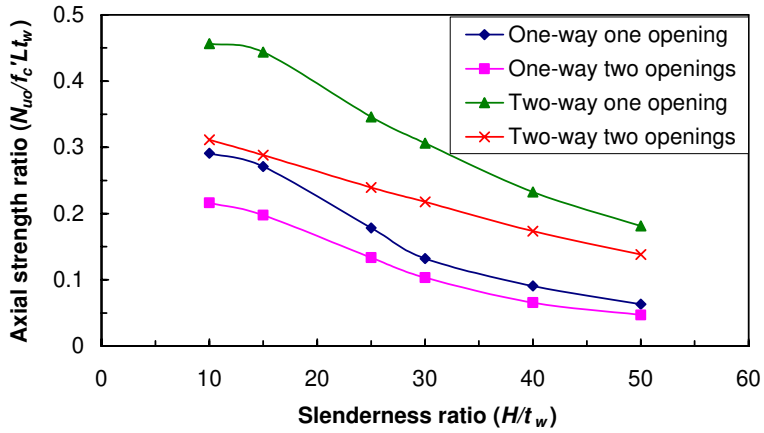

Figure 13. The effect of slenderness ratio on the axial strength ratio

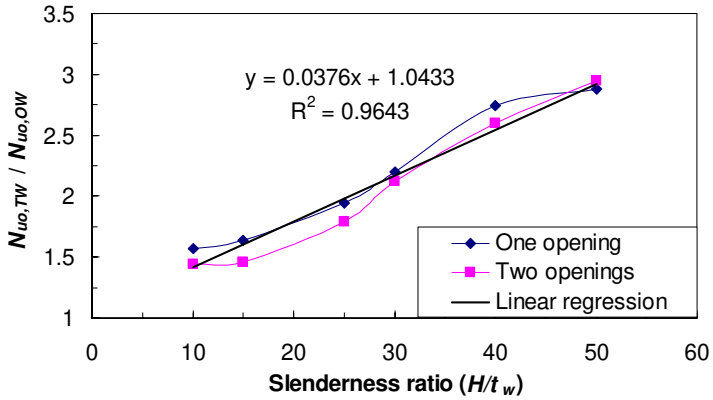

Figure 14. Relationship between H/t_w and additional strength gained from two-way restraints

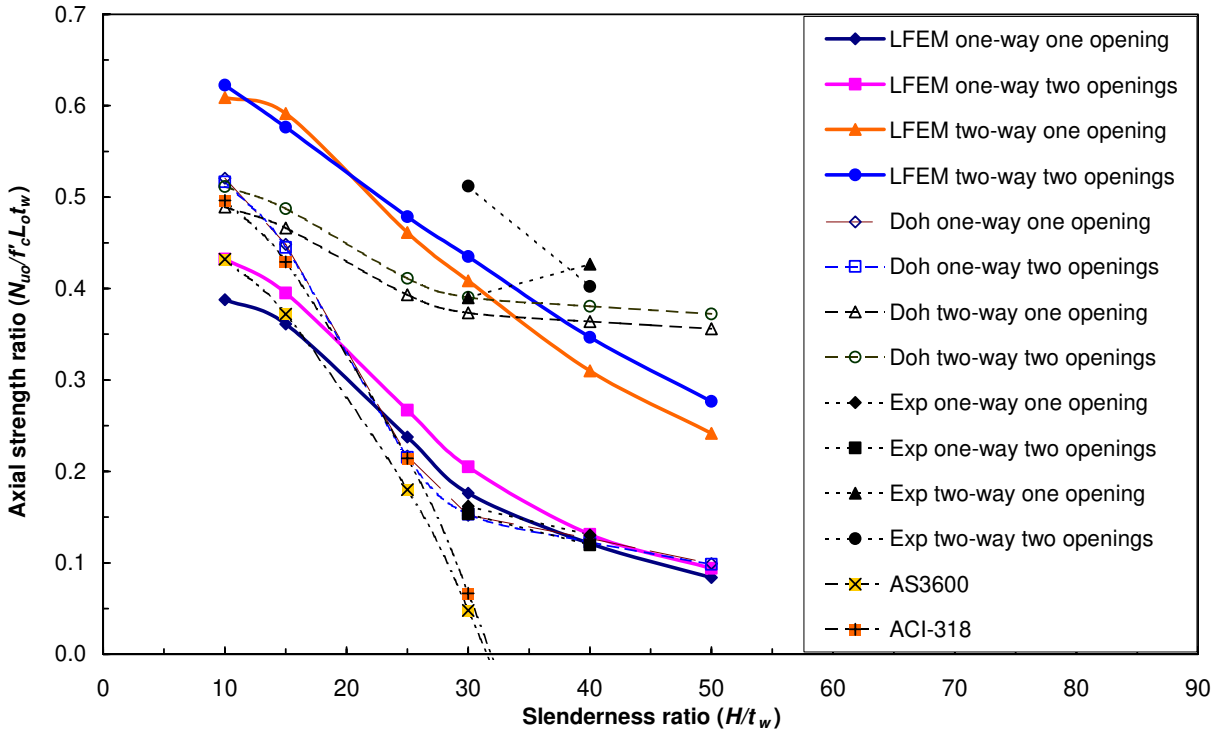

Figure 15. Comparison of LFEM results with other available data

(Experiment: Doh and Fragomeni 2004; Doh formula: Doh and Fragomeni 2006)

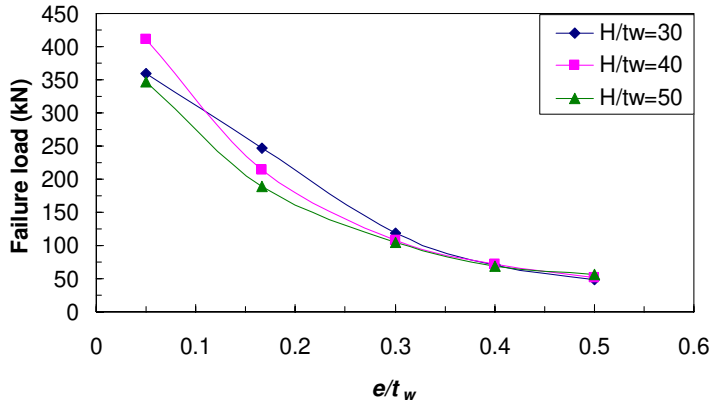

(a) one-way

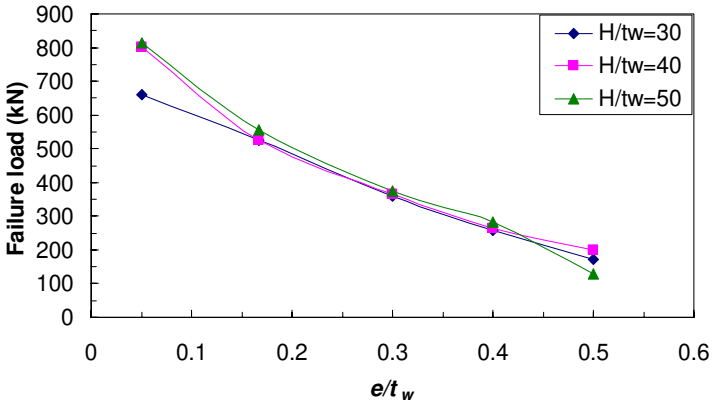

(b) two-way

Figure 16. Effect of eccentricity on failure load of wall panels

Table 1. Details of wall panels and convergence study results

Wall panel	Number of opening(s)	H and L (mm)	Slenderness ratio (H/t_w)	Size of opening (mm×mm)	f'_c (MPa)	Total number of nodes/elements
OW11	1	1200	30	300×300	53.0	253/72
OW12	1	1600	40	400×400	47.0	314/91
OW21	2	1200	30	300×300	50.0	270/75
OW22	2	1600	40	400×400	51.1	389/112
TW11	1	1200	30	300×300	50.3	253/72
TW12	1	1600	40	400×400	50.3	314/91
TW21	2	1200	30	300×300	50.3	270/75
TW22	2	1600	40	400×400	50.3	389/112

Note: OW – one-way; TW – two-way; first digit – number of opening(s); second digit – "1" for H/t_w = 30, "2" for H/t_w = 40.

Table 2. Comparison of experimental and LFEM failure loads for one-way walls

Wall panel	H and L (mm)	$N_{uo,Exp}$ (kN)	$N_{uo,LFEM}$ (kN)	$N_{uo,LFEM}/N_{uo,Exp}$
OW11	1200	309.02	336	1.09
OW12	1600	294.30	273	0.93
OW21	1200	185.41	247.5	1.33
OW22	1600	195.71	214.5	1.10
			Mean	1.11
			Standard deviation	0.17

Table 3. Comparison of experimental and LFEM failure loads for two-way walls

Wall panel	H and L (mm)	$N_{uo,Exp}$ (kN)	$N_{uo,LFEM}$ (kN)	$N_{uo,LFEM}/N_{uo,Exp}$
TW11	1200	750.47	739.5	0.99
TW12	1600	1030.05	748.5	0.73
TW21	1200	618.03	525	0.85
TW22	1600	647.46	558	0.86
			Mean	0.86
			Standard deviation	0.11

Table 4. Summary of failure load N_{uo} for one-way wall panels

Wall panel	Number of opening(s)	H and L (mm)	Opening size (mm)	H/t_w	$N_{uo,LFEM}$ (kN)	$N_{uo}/f'_c \cdot L \cdot t_w$
OW110	1	400	100	10	234	0.291
OW115		600	150	15	327	0.271
OW125		1000	250	25	358.5	0.178
OW130 (=OW11)		1200	300	30	336	0.132
OW140 (=OW12)		1600	400	40	273	0.091
OW150		2000	500	50	253.5	0.063
OW210	2	400	100	10	174	0.216
OW215		600	150	15	238.5	0.198
OW225		1000	250	25	268.5	0.133
OW230 (=OW21)		1200	300	30	247.5	0.103
OW240 (=OW22)		1600	400	40	214.5	0.066
OW250		2000	500	50	189	0.047

Note: OW – one-way; first digit – number of opening(s); last two digits – value for H/t_w.

Table 5. Summary of failure load N_{uo} for two-way wall panels

Wall panel	Number of opening(s)	H and L (mm)	Opening size (mm)	H/t_w	$N_{uo,LFEM}$ (kN)	$N_{uo}/f'_c \cdot L \cdot t_w$
TW110	1	400	100	10	367.5	0.457
TW115		600	150	15	535.5	0.444
TW125		1000	250	25	696	0.346
TW130 (=TW11)		1200	300	30	739.5	0.306
TW140 (=TW12)		1600	400	40	748.5	0.233
TW150		2000	500	50	729	0.181
TW210	2	400	100	10	250.5	0.311
TW215		600	150	15	348	0.288
TW225		1000	250	25	481.5	0.239
TW230 (=TW21)		1200	300	30	525	0.217
TW240 (=TW22)		1600	400	40	558	0.173
TW250		2000	500	50	556.5	0.138

Note: TW – two-way; first digit – number of opening(s); last two digits – value for H/t_w.

Table 6. Comparison of failure load N_{uo}

Wall panel	$N_{uo,Proposed}$ (kN)	$N_{uo,Exp}$ (kN)	$N_{uo,LFEM}$ (kN)	$N_{uo,proposed}/N_{uo,Exp}$	$N_{uo,proposed}/N_{uo,LFEM}$
OW110	314.19	–	234	–	1.34
OW115	405.82	–	327	–	1.24
OW125	327.28	–	358.5	–	0.91
OW130 (=OW11)	290.14	309.02	336	0.94	0.86
OW140 (=OW12)	285.89	294.3	273	0.97	1.05
OW150	299.33	–	253.5	–	1.18
OW210	207.94	–	174	–	1.20
OW215	268.59	–	238.5	–	1.13
OW225	216.61	–	268.5	–	0.81
OW230 (=OW21)	185.13	185.41	247.5	1.00	0.75
OW240 (=OW22)	200.62	195.71	214.5	1.03	0.94
OW250	198.11	–	189	–	1.05
TW110	443.00	–	367.5	–	1.21
TW115	649.32	–	535.5	–	1.21
TW125	648.01	–	696	–	0.93
TW130 (=TW11)	629.60	750.47	739.5	0.84	0.85
TW140 (=TW12)	729.01	1030.05	748.5	0.71	0.97
TW150	877.04	–	729	–	1.20
TW210	293.20	–	250.5	–	1.17
TW215	429.75	–	348	–	1.23
TW225	428.88	–	481.5	–	0.89
TW230 (=TW21)	401.73	618.03	525	0.65	0.77
TW240 (=TW22)	511.58	647.46	558	0.79	0.92
TW250	580.47	–	556.5	–	1.04
			Mean	0.87	1.04
		Standard	deviation	0.14	0.17

Table 7. Summary of eccentricity and failure load for one-way walls

Wall panel	H and L (mm)	H/t_w	e (mm)	$N_{uo,LFEM}$ (kN)	Maximum deflection (mm)
OW230e2	1200	30	2	360	9.51
OW230e6	1200	30	6.67	247.5	5.03
OW230e12	1200	30	12	118.5	3.62
OW230e16	1200	30	16	70.5	3.7
OW230e20	1200	30	20	48	3.12
OW240e2	1600	40	2	411	6.5
OW240e6	1600	40	6.67	214.5	5.85
OW240e12	1600	40	12	108	4.77
OW240e16	1600	40	16	72	4.18
OW240e20	1600	40	20	51	3.53
OW250e2	2000	50	2	346.5	7.64
OW250e6	2000	50	6.67	189	7.12
OW250e12	2000	50	12	105	6.35
OW250e16	2000	50	16	69	4.12
OW250e20	2000	50	20	55.5	4.69

Note: OW – one-way; first digit – number of openings; second and third digits – value for H/t_w; e – eccentricity; last digit(s) – eccentricity in mm.

Table 8. Summary of eccentricity and failure load for two-way walls

Wall panel	H and L (mm)	H/t_w	e (mm)	$N_{uo,LFEM}$ (kN)	Maximum deflection (mm)
TW230e2	1200	30	2	660	8.32
TW230e6	1200	30	6.67	525	5.8
TW230e12	1200	30	12	360	7.61
TW230e16	1200	30	16	259.5	8.86
TW230e20	1200	30	20	171	7.47
TW240e2	1600	40	2	801	5.85
TW240e6	1600	40	6.67	525	5.8
TW240e12	1600	40	12	364.5	5.51
TW240e16	1600	40	16	265.5	5.71
TW240e20	1600	40	20	199.5	9.41
TW250e2	2000	50	2	814.5	7.71
TW250e6	2000	50	6.67	556.5	12.39
TW250e12	2000	50	12	375	1.24
TW250e16	2000	50	16	283.5	1.06
TW250e20	2000	50	20	129	1.95

Note: TW – two-way; first digit – number of openings; second and third digits – value for H/t_w; e – eccentricity; last digit(s) – eccentricity in mm.